Skeletal Radiology (2019) 48:1261–1268
https://doi.org/10.1007/s00256-019-3150-6

TECHNICAL REPORT

Optimizing radiation dose parameters in MDCT arthrography of the shoulder: illustration of basic concepts in a cadaveric study

Julien Aguet[1] · Fabio Becce[1] · Vincent Dunet[1] · Alain Vlassenbroek[2] · Emmanuel E. Coche[3] · Patrick Omoumi[1]

Received: 20 August 2018 / Revised: 11 December 2018 / Accepted: 7 January 2019 / Published online: 6 February 2019

Abstract

Objective To determine in a cadaveric study the lowest achievable radiation dose and optimal tube potential generating diagnostic image quality in multidetector computed tomography (MDCT) arthrography of the shoulder.

Materials and methods Six shoulders from three human cadavers were scanned using a 256-MDCT system after intra-articular injection of diluted iodinated contrast material. Using six decreasing radiation dose levels ($CTDI_{vol}$: 20, 15, 10, 8, 6, and 4 mGy) and for each dose level, four decreasing tube potentials (140, 120, 100, and 80 kVp), image noise and contrast-to-noise ratio (CNR) were measured. Two independent and blinded observers assessed the overall diagnostic image quality, subjective amount of noise, and severity of artifacts according to a four-point scale. Influence of those MDCT data acquisition parameters on objective and subjective image quality was analyzed using the Kruskal–Wallis and Wilcoxon signed-rank tests, and pairwise comparisons were performed.

Results Multidetector CT protocols with radiation doses of 15 mGy or higher, combined with tube potentials of 100 kVp or higher, were equivalent in CNR to the reference 20 mGy–140 kVp protocol (all $p \geq 0.054$). Above a $CTDI_{vol}$ of 10 mGy and a tube potential of 120 kVp, all protocols generated diagnostic image quality and subjective noise equivalent to the 20 mGy–140 kVp protocol (all $p \geq 0.22$).

Conclusions Diagnostic image quality in MDCT arthrography of the shoulder can be obtained with a radiation dose of 10 mGy at an optimal tube potential of 120 kVp, corresponding to a reduction of up to 50% compared with standard-dose protocols, and as high as 500% compared with reported protocols in the literature.

Keywords MDCT · CT · Shoulder · Arthrography · Radiation dose · Image quality

Introduction

Multidetector computed tomography (MDCT) arthrography of the shoulder is an effective and reliable alternative to magnetic resonance imaging (MRI) and MR arthrography for the diagnosis of various internal derangements of the shoulder. It is typically used in patients with contraindications to MRI, after previously failed MRI attempts, such as in patients with claustrophobia, or simply when MRI is not available [1–6]. Moreover, despite recent advances in metal artifact reduction with MRI [7], MDCT arthrography is still considered the reference standard in the postoperative setting, particularly after shoulder arthroplasty [8].

However, there are downsides to this imaging technique, mainly the need for injection of iodinated contrast material and the exposure to ionizing radiation. This is all the more true for the shoulder joint, owing to the proximity of radiosensitive organs, such as the thyroid gland and the lungs [9–13].

To the best of our knowledge, no studies have been published that focus on the optimization of radiation dose in MDCT arthrography of the shoulder. Reports from the literature show great variability between both data acquisition and image reconstruction protocols. Although some perform shoulder MDCT arthrography at 140 kVp, others use a tube potential of 120 kVp. A wide range of reported radiation doses (expressed in volume CT dose index [$CTDI_{vol}$]) can be found in the literature, from

✉ Patrick Omoumi
patrick.omoumi@chuv.ch

[1] Department of Diagnostic and Interventional Radiology, Lausanne University Hospital and University of Lausanne, Rue du Bugnon 46, 1011 Lausanne, Switzerland

[2] Philips Healthcare, Rue des Deux Gares 80, 1070 Bruxelles, Belgium

[3] Department of Radiology and Medical Imaging, Cliniques Universitaires Saint-Luc, Université Catholique de Louvain, Avenue Hippocrate 10, 1200 Bruxelles, Belgium

10.1 mGy to 51 mGy [14, 15]. For the European Union, suggested $CTDI_{vol}$ is 15 mGy or lower [16]. According to the Swiss Federal Office of Public Health, the reference dose in Switzerland is $CTDI_{vol}$ 30 mGy and the target dose is 15 mGy [17].

The radiation dose delivered by MDCT is influenced by both the tube potential (expressed in kVp) and the tube current–time product (expressed in mAs). The tube potential in particular is a critical parameter for protocol optimization as it influences radiation dose exponentially, and is also a major determinant of image contrast through the photoelectric effect, especially when imaging high-Z materials such as iodine and, to a lesser extent, cortical bone [18–20]. Although there is a growing interest in developing technology aimed at reducing radiation dose by targeting various approaches, especially in terms of post-processing, tube parameters remain a fundamental part of protocol optimization.

Our purpose was to illustrate the influence of these basic concepts and to determine, in a cadaveric study, the combination of radiation dose level ($CTDI_{vol}$) and tube potential (kVp) yielding the lowest possible dose while still providing diagnostic image quality in shoulder MDCT arthrography.

Materials and methods

The institutional ethics committee approved this single-center cadaveric study.

Study population

We examined six shoulder joints from three fresh human cadavers with nontraumatic-related causes of death (one male, two females, mean age 77.3 ± 8 years; mean weight 72.8 ± 14.5 kg, range 58–87 kg) provided to us by our anatomy laboratory (Laboratoire d'anatomie humaine, pôle de morphologie [MORF], Institut de recherche clinique et expérimentale [IREC], Faculté de médecine de l'Université catholique de Louvain).

Arthrography technique

The same musculoskeletal radiologist with 5 years of experience performed all the examinations. Using an anterior approach under MDCT guidance, all six glenohumeral joints were injected with 10 ml of diluted iodinated contrast material (one-part ioxaglate [Hexabrix 320; Guerbet, Villepinte, France] and one-part normal saline) using a 22-gauge needle.

MDCT arthrography protocol

Cadavers were placed head first in supine position, arms along the body, with glenohumeral joints in neutral position. MDCT arthrograms were obtained scanning from the top of the acromioclavicular joint to the lower margin of the axillary recess of the glenohumeral joint using a 256-MDCT scanner (Brilliance iCT; Philips Healthcare, Best, The Netherlands). Each cadaver was scanned 24 times using the helical mode with varying $CTDI_{vol}$ and tube potential parameters, starting from a $CTDI_{vol}$ of 20 mGy, and decreasing to 15, 10, 8, 6, and 4 mGy. At each dose level, four tube potentials were selected, starting from 140 kVp, and decreasing to 120, 100, and 80 kVp. The $CTDI_{vol}$, kVp, and corresponding mAs for the 24 acquisitions on each shoulder are reported in Table 1. The remaining data acquisition parameters were identical for each scan, with a focal spot size of 0.6 × 0.7 mm, exposure time of 2.463 s, beam collimation of 64 × 0.625 mm, beam pitch of 0.2, and a scanning field of view of 40 × 40 cm. Images were reconstructed using a three-dimensional cone-beam filtered-back-projection algorithm, a high-spatial-resolution kernel, a section thickness of 0.9 mm with a 0.45-mm section overlap, and a 768 × 768 matrix.

Objective image quality

Measurements were performed by a 4th-year radiology resident on a workstation equipped with a picture archiving and

Table 1 Multidetector computed tomography acquisition protocol for the 24 scans performed on each shoulder

CTDI (mGy)	kVp	mAs
20	140	200
20	120	300
20	100	493
20	80	1,032
15	140	140
15	120	209
15	100	350
15	80	724
10	140	100
10	120	150
10	100	246
10	80	515
8	140	81
8	120	121
8	100	197
8	80	414
6	140	57
6	120	91
6	100	145
6	80	308
4	140	39
4	120	57
4	100	99
4	80	207

communication system (PACS) (Vue, version 11.4; Carestream Health, Rochester, NY, USA). Two circular regions of interest (ROI) of 30 mm^2 and 50 mm^2 were placed within the iodinated contrast material in the glenohumeral joint and the deltoid muscle respectively, avoiding potential areas of beam hardening and photon starvation artifacts (Fig. 1). Measurements were considered on three consecutive axial sections, and mean values in Hounsfield units (HU) and standard deviations (SD) were recorded. The two ROIs were first placed on the images from the MDCT protocol with the highest dose (20 mGy) and then copy-pasted onto the corresponding registered images from the protocols with the lower doses. Noise was defined as the SD of the ROI in the muscle. The contrast-to-noise ratio (CNR) was calculated using the following formula:

$$CNR = \frac{(mean\ HU_{contrast\ material} - mean\ HU_{muscle})}{SD_{muscle}}$$

Subjective image quality

All shoulder MDCT arthrograms were independently reviewed by two musculoskeletal radiologists with 5 and 3 years of experience at the time of the study. One radiology resident displayed the image series for each dose level separately to each observer, in random order, blinded for patient characteristics and acquisition parameters. Images were viewed in a nonreformatted axial plane with a section thickness of 0.9 mm, zoomed in on the glenohumeral joint by a factor of 330% (30 × 20 cm display field of view), with a window width and center of 500 and 2,500 HU respectively.

Observers performed a semiquantitative analysis of images for each dose level, rating the overall diagnostic image quality, subjective amount of noise, and severity of artifacts based on a four-point scale (4 = exemplary, 3 = diagnostic, 2 = limited, and 1 = nondiagnostic) developed by the Radiological Society of North America [21]. Severity of artifacts was assessed by evaluating the amount of hypoattenuations and streak artifacts, focusing on areas surrounding joint cavities (especially the subscapular and axillary recesses), or bone structures. The subjective amount of noise was assessed by analyzing the grain of the image in homogeneous parts of the shoulder, including subcutaneous fatty tissue and non-atrophic muscle bodies. Overall diagnostic image quality was assessed by analyzing the conspicuity of articular surfaces (including cartilage surfaces and rotator cuff tendons), muscular internal structures, and cortical and trabecular bone structures.

Statistical analysis

Statistical analysis was performed using Stata 13.1 software (StataCorp, College Station, TX, USA). Continuous variables are displayed as mean ± SD. Categorical variables are presented as numbers or proportions. For subjective image quality parameters, inter- and intraobserver agreement was assessed using kappa statistics (with linear weight) and interpreted according to the Landis and Koch grading system [22]. To assess intraobserver agreement, 25 scans (out of the 144 scans acquired in total) were randomly selected and assessed by one of the observers in a second session, with an interval of at least 3 months. Mean values calculated by averaging the scores of the two observers were used for further analyses.

Objective image quality (CNR) and subjective image quality (overall quality, noise, and artifacts) parameters were compared using the nonparametric Kruskal–Wallis and Wilcoxon signed-rank tests. Pairwise comparison of objective and subjective image quality parameters was also performed using the Goldstein test to find the set of parameters with the lowest dose that were equivalent to the 20 mGy–140 kVp MDCT

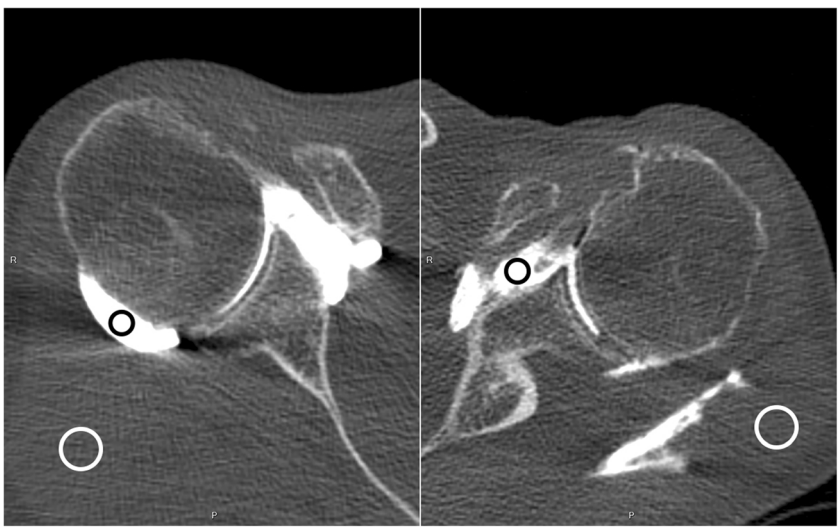

Fig. 1 Right and left shoulder CT arthrograms of the same cadaver showing schematic representation of the circular ROIs placed within the iodinated contrast material in the glenohumeral joint (*black circle*) and the deltoid muscle (*white circle*) respectively. Note the presence of iodinated contrast material posteriorly, superficial to the infraspinatus tendon and muscle on the left shoulder (*right image*), as a result of a full-thickness tear of the supraspinatus tendon (not shown)

protocol. The effect of $CTDI_{vol}$ and kVp on objective image quality was additionally assessed using the Spearman rho coefficient. A significance level of $p \leq 0.05$ was considered for all tests.

Results

Objective image quality

The CNR significantly increased with increasing levels of $CTDI_{vol}$ and kVp (rho = 0.71, $p < 0.0001$ and rho = 0.43, $p < 0.0001$ respectively; Fig. 2).

For each level of $CTDI_{vol}$, there was statistical equivalence in CNR between 120 kVp and 140 kVp (all $p \geq 0.52$ [test of difference], all $p \geq 0.77$ [test of equivalence]).

Pairwise comparisons showed that MDCT protocols with radiation dose levels of 15 mGy or higher, combined with tube potentials of 100 kVp or higher, were equivalent in CNR to the reference 20 mGy–140 kVp protocol (all $p \geq 0.054$). No 80-kVp protocol was statistically equivalent to the 20 mGy–140 kVp protocol (all $p \leq 0.0022$).

Subjective image quality

Inter- and intraobserver agreement

Interobserver agreement was fair for all three subjective image quality parameters (0.35, 0.55, and 0.38 for overall image quality, subjective noise, and image artifacts respectively). Despite differences in the subjective evaluation of images between readers, the trends in the scoring of all three parameters were similar.

Intraobserver agreement was substantial to almost perfect (0.85, 0.75, and 0.92 for overall image quality, subjective noise and image artifacts respectively).

Overall image quality

For each $CTDI_{vol}$ level, the qualitative analysis showed statistical equivalence in overall image quality between tube potentials of 120 kVp and 140 kVp (all $p \geq 0.14$ [test of difference], all $p \geq 0.15$ [test of equivalence]; Fig. 3).

Pairwise comparisons showed that MDCT protocols with dose levels of 10 mGy or higher, combined with tube potentials of 120 kVp or higher, were equivalent in overall image quality to the reference 20 mGy–140 kVp protocol (all $p \geq 0.22$). No 80-kVp protocol was statistically equivalent to the 20 mGy–140 kVp protocol (all $p \leq 0.0079$). Above a $CTDI_{vol}$ of 10 mGy and a tube potential of 120 kVp, all protocols generated diagnostic image quality images equivalent to the 20 mGy–140 kVp protocol (all $p \geq 0.22$).

Subjective noise

For each $CTDI_{vol}$ level, the qualitative analysis showed statistical equivalence in subjective noise between tube potentials of 120 kVp and 140 kVp (all $p \geq 0.14$ [test of difference], all $p \geq 0.14$ [test of equivalence]; Fig. 4a).

Pairwise comparisons showed that MDCT protocols with dose levels of 10 mGy or higher, combined with tube potentials of 120 kVp or higher, were equivalent in subjective noise to the reference 20 mGy–140 kVp protocol (all $p \geq 0.49$). In

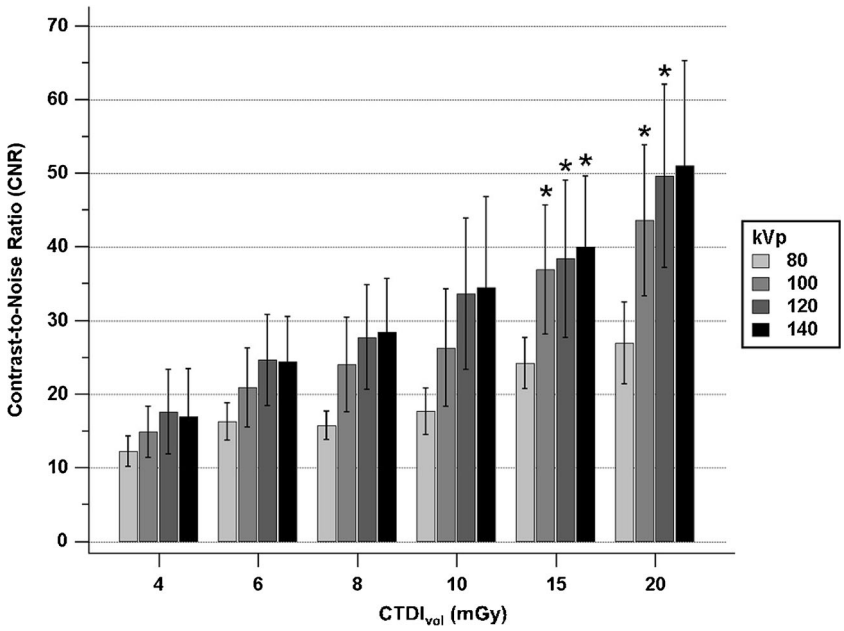

Fig. 2 Clustered bar chart showing a statistically significant linear trend for an increase in CNR with increasing levels of radiation dose. Each cluster corresponds to one level of radiation dose ($CTDI_{vol}$, in mGy), with varying levels of tube potential (ranging from 80 to 140 kVp). *Asterisks* indicate MDCT data acquisition protocols providing CNR statistically equivalent to the reference 20 mGy–140 kVp protocol in pairwise comparisons

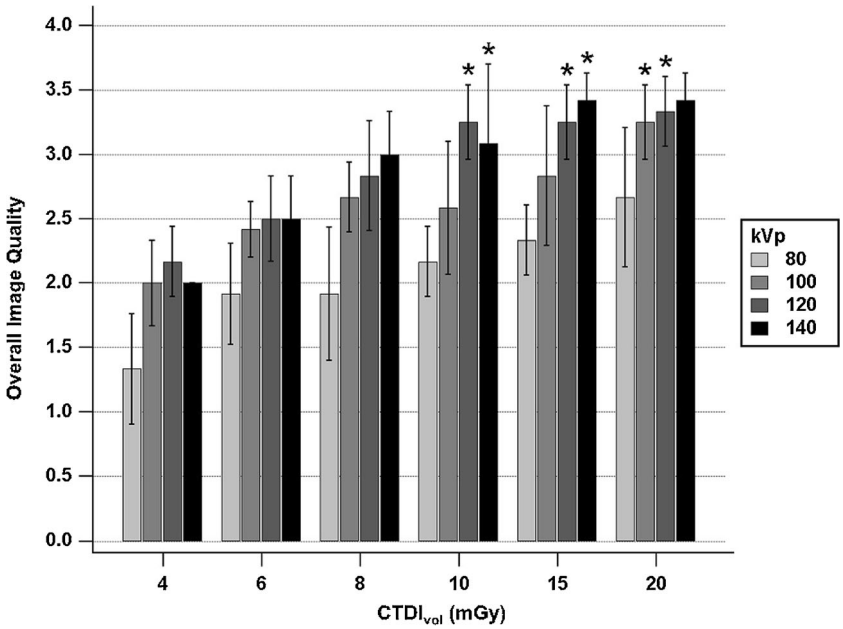

Fig. 3 Clustered bar chart showing the overall image quality, based on the appearance of the glenohumeral cartilage surfaces, rotator cuff tendons, and the cortical and trabecular bone structures, relative to $CTDI_{vol}$ (mGy) and tube potential (kVp). Increasing $CTDI_{vol}$ and kVp is significantly associated with increasing image quality from 4 to 10 mGy, and from 80 to 140 kVp. *Asterisks* indicate MDCT data acquisition protocols providing image quality statistically equivalent to the reference 20 mGy–140 kVp protocol in pairwise comparisons

addition, protocols with $CTDIs_{vol}$ of 8 mGy at 140 kVp, or 20 mGy at 80 kVp and 100 kVp, were equivalent in subjective noise to the 20 mGy–140 kVp protocol (all $p \geq 0.057$).

Artifacts

For each $CTDI_{vol}$ level, the qualitative analysis showed statistical equivalence in subjective evaluation of hypoattenuations and streak artifacts between tube potentials of 120 kVp and 140 kVp (all $p \geq 0.14$ [test of difference], all $p \geq 0.15$ [test of equivalence]; Fig. 4b).

Pairwise comparisons showed that MDCT protocols with dose levels of 6 mGy or higher, combined with tube potentials of 100 kVp or higher, were equivalent in subjective evaluation of artifacts to the reference 20 mGy–140 kVp protocol (all $p \geq 0.074$). In addition, protocols with a $CTDI_{vol}$ of 4 mGy combined with tube potentials of 120 kVp or higher were equivalent in subjective evaluation of artifacts to the 20 mGy–140 kVp protocol (all $p > 0.09$). No 80-kVp protocol was statistically equivalent to the 20 mGy–140 kVp protocol (all $p \leq 0.017$).

Discussion

In this study, we demonstrated that overall diagnostic image quality in MDCT arthrography of the shoulder could be obtained with a radiation dose of 10 mGy, combining an optimal tube potential of 120 kVp and 150 mAs corresponding to a reduction of up to 50% compared with standard-dose protocols (20 mGy, 140 kVp, 200 mAs), and as high as 500% compared with reported protocols in the literature (estimated $CTDI_{vol}$ of 51 mGy, obtained with 140 kVp and 350 mAs [15]). To the best of our knowledge, this is the first study aimed at optimizing the radiation dose of shoulder MDCT arthrography by separately and systematically assessing the influence of key MDCT data acquisition parameters, such as the tube potential and tube current–time product.

The diagnostic tasks performed with MDCT arthrography mainly involve objects that present inherently high contrast between them, such as intra-articular contrast medium and surrounding articular tissues (i.e., tendons, cartilage, labroligamentous complex), and require high spatial resolution. In this context, it has been shown that higher noise levels can be tolerated without affecting the diagnostic value of the images, yet up to a certain limit, that depends on the clinical task (contrast difference [ΔHU] and size of the lesion) [23]. This is supported by the results of our study: although there was a significant difference in CNR of images obtained at 10 and 15 mGy, the subjective image quality assessment (specifically for overall image quality and subjective noise) showed statistical equivalence between acquisitions at 10 and 20 mGy. This was further supported in an in vitro study focusing on the evaluation of articular cartilage in hip MDCT arthrography, which showed that the effective dose can be significantly reduced (to as low as 0.5 mSv) without affecting image quality [19, 24–26].

Apart from the optimization of the radiation dose in general, it is also important to optimize the tube potential when dealing with MDCT arthrography. In fact, tube potential is one of the main determinants of image contrast through the photoelectric effect, which is mostly visible in the presence of high Z-materials, such as iodine and, to a lesser extent, cortical bone. Indeed, when reducing the tube potential, the attenuation of high-Z materials increases in comparison to low-Z materials, such as soft tissues, hereby increasing image

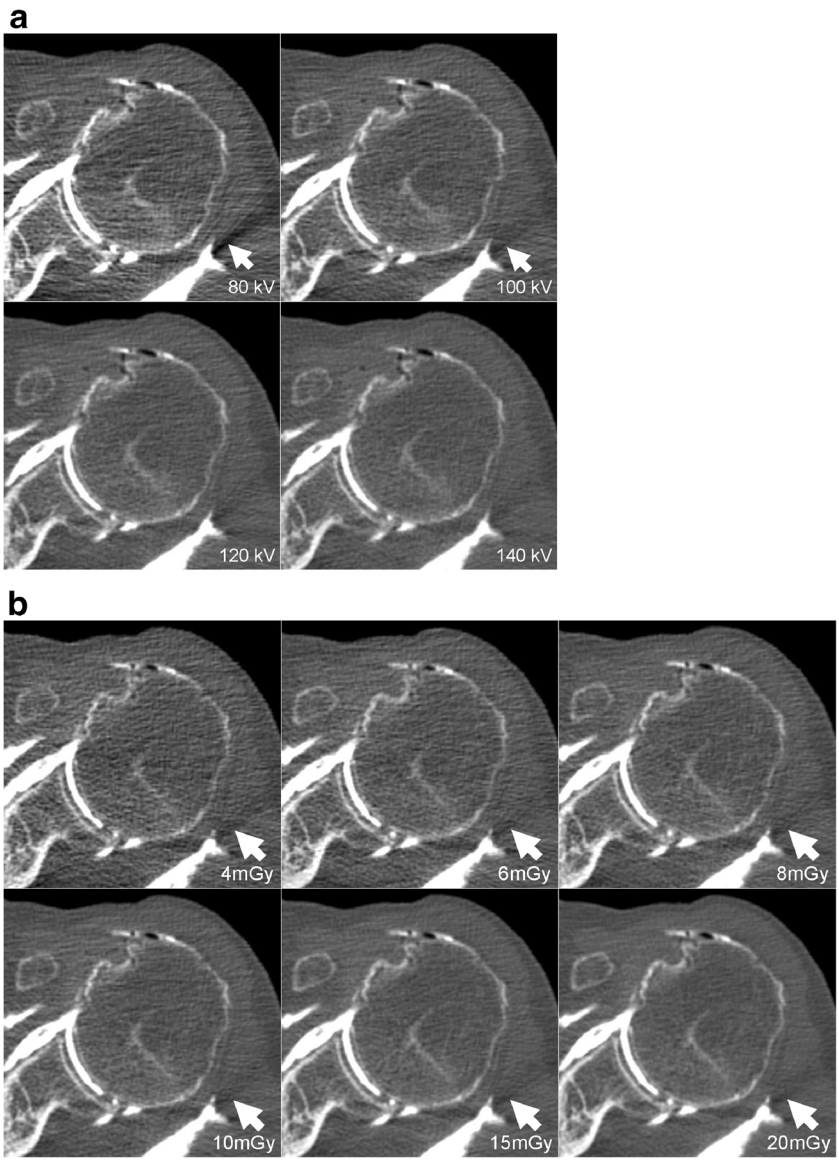

Fig. 4. **a** Examples of image quality increasing when radiation dose was kept stable at 10 mGy but tube potential increased from 80 to 140 kVp. With window width and center kept constant, there is a significant decrease in overall image contrast, and decreasing streaking artifacts with increasing kVp (*arrows*). The last two images were considered to be of diagnostic quality. **b** Examples of image quality increasing when tube potential was kept stable at 120 kVp but radiation dose increased from 4 to 20 mGy. Although image noise significantly increases with increasing dose level, the last three images obtained at 10, 15, and 20 mGy were all considered to be of diagnostic quality. Of note, there is no difference in the appearance of streaking artifacts (*arrows*) among the six images, all acquired at a tube potential of 120 kVp. Window width and center were kept constant across all figure parts

contrast [19, 20, 27]. This property can be used to keep the CNR constant while reducing radiation dose, through a reduction in tube potential. The photoelectric effect can also be used to decrease the concentration of contrast material to be injected in arthrographic procedures, which has been shown with the use of dual-energy CT [27]. However, decreasing tube potential is associated with drawbacks, in particular an increase in image noise and beam hardening (hypoattenuations) artifacts. Therefore, it is important to optimize the tube potential to find a trade-off between image contrast, image noise, and beam hardening artifacts. In one study that previously addressed this issue, Ahn et al. [28] prospectively showed on 54 MDCT arthrograms of the shoulder that reducing the tube potential from 140 to 120 kVp, while maintaining tube current–time product constant at 200 mAs, leads to a decrease in the radiation dose of 33%, while maintaining subjective image quality [28].

Our results are in line with this previous report as we confirmed the equivalence of objective and subjective image quality between 120 and 140 kVp for all the $CTDI_{vol}$ levels investigated. In the lower range, our results have shown that below 100 kVp, beam hardening artifacts have a significantly

negative impact on image quality, contrasting with imaging of peripheral joints for which tube potentials as low as 80 kVp can be used [10, 19]. Of note, automatic kilovoltage selection has recently become available on certain clinical MDCT scanners, allowing the choice of the optimal potential depending on the patient's attenuation profile and the diagnostic task (low-contrast versus high-contrast objects [29]). These modules have not yet been evaluated for MDCT arthrography of the shoulder.

When optimizing the MDCT data acquisition protocol, other parameters apart from tube potential and current–time product have to be taken into account [10, 19]. These classically include not only factors to consider during the acquisition, such as keeping the scan length to a minimum required for the diagnostic task, positioning the patient to minimize the body parts present in the acquisition field (i.e., elevating the contralateral shoulder in the z-axis), but also factors that come into play after the acquisition [19]. Increasing the reconstruction slice thickness is a simple way of decreasing image noise, which is particularly useful for low-contrast structures. Moreover, iterative reconstructions have more recently been used to improve image quality for various musculoskeletal applications [19, 30–34]. By considering certain factors, such as statistical models and modeling of MDCT system optics, iterative reconstructions allow a drastic reduction in image noise compared with standard filtered-back projection (FBP) techniques that were used in this study. Therefore, iterative reconstructions can be used to reduce radiation dose, while keeping the image quality constant. By applying iterative reconstructions (specifically adaptive statistical iterative reconstruction) to MDCT arthrography of the hip, it has been shown that radiation dose can be reduced by approximately 35–60%, while maintaining diagnostic image quality compared with standard FBP techniques for the assessment of acetabular labrum tears and articular cartilage lesions [34]. Furthermore, iterative reconstruction techniques can reduce certain artifacts such as photon starvation artifacts [19]. The application of such protocols in addition to our multiparameter optimization may allow even further dose reduction in MDCT arthrography of the shoulder.

Our study has some limitations to consider. First, the study population contained only a small number of specimens (six shoulders from three cadavers). Second, although we did not assess the impact of body size on photon starvation, known to be an issue when reducing radiation dose, we did evaluate cadavers with weights ranging from 58 to 86.5 kg, with a mean of 77.3 kg, reflecting the range encountered in our practice. Our results, therefore, may not apply to patients who are not of standard size. For very large patients, it may sometimes be necessary to keep the tube potential at 140 kVp, especially in the presence of the bony skeleton at the level of the shoulder girdle [10]. On the other hand, for smaller adults, radiation dose may be reduced even further. As discussed above, the application of automatic kilovoltage selection protocols to shoulder CT arthrography may help in this task [29]. Furthermore, the use of automatic tube current modulation could allow image quality to be kept constant by adapting radiation dose to the patient habitus, thereby potentially reducing radiation doses further for thinner patients [29]. Third, we demonstrated the feasibility of significantly reducing dose in regard to image quality only and did not assess the impact on diagnostic performance. The imaged shoulders showed evidence of pathological conditions, including rotator cuff and cartilage lesions. However, these lesions were visible even at the lowest radiation dose levels, thus hindering any comparison of the conspicuity of pathological conditions between protocols. This can be explained by the high tolerance to image noise with high-contrast diagnostic tasks [19]. Although below a certain limit, some images were judged inadequate in the subjective analysis, a larger number of cadavers would be required to demonstrate an impact on diagnostic performance. Finally, we injected a concentration of iodinated contrast material that is used routinely in clinical practice [2, 5]. Other concentrations of contrast material could affect the image quality, in particular streaking artifacts. This parameter was not taken into account in this study.

In conclusion, we demonstrated that diagnostic quality imaging in MDCT arthrography of the shoulder is feasible with a reduction of up to 50% in radiation dose compared with standard-dose protocols, and as high as 500% compared with reported protocols in the literature, by applying an optimal tube voltage of 120 kVp. We hereby illustrate some important concepts that should be considered when optimizing acquisition protocols with CT arthrography, in particular, the importance of reducing tube voltage to 120 kVp in standard-size patients, and the notion that higher noise levels can be tolerated because of the high-contrast task at hand. These concepts should be used to guide the optimization of MDCT arthrography protocols for future clinical and research studies.

Acknowledgments We would like to thank the Anatomy Lab of the Cliniques Universitaires Saint-Luc, Université Catholique de Louvain, for providing us with the cadavers.

Compliance with ethical standards

Conflicts of interest None.

References

1. Fritz J, Fishman EK, Small KM, Winalski CS, Horger MS, Corl F, et al. MDCT arthrography of the shoulder with datasets of isotropic

resolution: indications, technique, and applications. Am J Roentgenol. 2012;198(3):635–46.
2. Omoumi P, Bafort A-C, Dubuc J-E, Malghem J, Vande Berg BC, Lecouvet FE. Evaluation of rotator cuff tendon tears: comparison of multidetector CT arthrography and 1.5-T MR arthrography. Radiology. 2012;264(3):812–22.
3. Acid S, Le Corroller T, Aswad R, Pauly V, Champsaur P. Preoperative imaging of anterior shoulder instability: diagnostic effectiveness of MDCT arthrography and comparison with MR arthrography and arthroscopy. Am J Roentgenol. 2012;198(3):661–7.
4. Lecouvet FE, Simoni P, Koutaïssoff S, Vande Berg BC, Malghem J, Dubuc J-EE. Multidetector spiral CT arthrography of the shoulder. Clinical applications and limits, with MR arthrography and arthroscopic correlations. Eur J Radiol. 2008;68(1):120–36.
5. Omoumi P, Rubini A, Dubuc JE, Vande Berg BC, Lecouvet FE. Diagnostic performance of CT-arthrography and 1.5T MR-arthrography for the assessment of glenohumeral joint cartilage: a comparative study with arthroscopic correlation. Eur Radiol. 2015;25(4):961–9.
6. Omoumi P, Mercier GA, Lecouvet F, Simoni P, Vande Berg BC. CT arthrography, MR arthrography, PET, and scintigraphy in osteoarthritis. Radiol Clin N Am. 2009;47(4):595–615.
7. Jungmann PM, Agten CA, Pfirrmann CW, Sutter R. Advances in MRI around metal. J Magn Reson Imaging. 2017;46(4):972–91.
8. Mallo GC, Burton L, Coats-Thomas M, Daniels SD, Sinz NJ, Warner JJP. Assessment of painful total shoulder arthroplasty using computed tomography arthrography. J Shoulder Elbow Surg. 2015;24(10):1507–11. https://doi.org/10.1016/j.jse.2015.06.027.
9. Biswas D, Bible JE, Bohan M, Simpson AK, Whang PG, Grauer JN. Radiation exposure from musculoskeletal computerized tomographic scans. J Bone Joint Surg Am. 2009;91(8):1882–9.
10. Gervaise A, Teixeira P, Villani N, Lecocq S, Louis M, Blum A. CT dose optimisation and reduction in osteoarticular disease. Diagn Interv Imaging. 2013;94(4):371–88.
11. Guggenberger R, Ulbrich EJ, Dietrich TJ, Scholz R, Kaelin P, Köhler C, et al. C-arm flat-panel CT arthrography of the shoulder: radiation dose considerations and preliminary data on diagnostic performance. Eur Radiol. 2017;27(2):454–63.
12. Sinnott B, Ron E, Schneider AB. Exposing the thyroid to radiation: a review of its current extent, risks, and implications. Endocr Rev. 2010;31(5):756–73.
13. Mazonakis M, Tzedakis A, Damilakis J, Gourtsoyiannis N. Thyroid dose from common head and neck CT examinations in children: is there an excess risk for thyroid cancer induction? Eur Radiol. 2007;17(5):1352–7.
14. Waldt S, Metz S, Burkart A, Mueller D, Bruegel M, Rummeny EJ, et al. Variants of the superior labrum and labro-bicipital complex: a comparative study of shoulder specimens using MR arthrography, multi-slice CT arthrography and anatomical dissection. Eur Radiol. 2006;16(2):451–8.
15. De Maeseneer M, Boulet C, Pouliart N, Kichouh M, Buls N, Verhelle F, et al. Assessment of the long head of the biceps tendon of the shoulder with 3T magnetic resonance arthrography and CT arthrography. Eur J Radiol. 2012;81(5):934–9. https://doi.org/10.1016/j.ejrad.2011.01.121.
16. Bongartz G, Golding SJ, Jurik AG, Leonardi M, van Persijn van Meerten E, Geleijns J, et al. European guidelines on quality criteria for computed tomography. March 2004. Available from: http://www.drs.dk/guidelines/ct/quality/mainindex.htm.
17. FOPH Swiss Federal Office of Public Health. Notice R-06-06. Ref R-06-06df. Established 01.04.2010.
18. Omoumi P, Becce F, Ott JG, Racine D, Verdun FR. Optimization of radiation dose and image quality in musculoskeletal CT: emphasis on iterative reconstruction techniques I. Semin Musculoskelet Radiol. 2015;19(5):415–21.
19. Omoumi P, Verdun FR, Becce F. Optimization of radiation dose and image quality in musculoskeletal CT: emphasis on iterative reconstruction techniques II. Semin Musculoskelet Radiol. 2015;19(5):422–30.
20. Omoumi P, Becce F, Racine D, Ott JG, Andreisek G, Verdun FR. Dual-energy CT: basic principles, technical approaches, and applications in musculoskeletal imaging I. Semin Musculoskelet Radiol. 2015;19(5):431–7.
21. Radiological Society of North America. RadLex: a lexicon for uniform indexing and retrieval of radiology information resources [Internet]. March 2018. Available from: http://radlex.org/.
22. Landis JR, Koch GG. The measurement of observer agreement for categorical data. Biometrics. 1977;33(1):159–74.
23. Racine D, Viry A, Becce F, Schmidt S, Ba A, Bochud FO, et al. Objective comparison of high-contrast spatial resolution and low-contrast detectability for various clinical protocols on multiple CT scanners. Med Phys. 2017;44(9):e153–63.
24. Simoni P, Leyder PP, Albert A, Malchair F, Maréchal C, Scarciolla L, et al. Optimization of computed tomography (CT) arthrography of hip for the visualization of cartilage: an in vitro study. Skeletal Radiol. 2014;43(2):169–78.
25. Roth TD, Buckwalter KA, Choplin RH. Musculoskeletal computed tomography: current technology and clinical applications. Semin Roentgenol. 2013;48(2):126–39. https://doi.org/10.1053/j.ro.2012.11.009.
26. Gurung J, Khan MF, Maataoui A, Herzog C, Bux R, Bratzke H, et al. Multislice CT of the pelvis: dose reduction with regard to image quality using 16-row CT. Eur Radiol. 2005;15(9):1898–905.
27. Subhas N, Freire M, Primak AN, Polster JM, Recht MP, Davros WJ, et al. CT arthrography: in vitro evaluation of single and dual energy for optimization of technique. Skeletal Radiol. 2010;39(10):1025–31.
28. Ahn SJ, Hong SH, Chai JW, Choi J-YY, Yoo HJ, Kim SH, et al. Comparison of image quality of shoulder CT arthrography conducted using 120 kVp and 140 kVp protocols. Korean J Radiol. 2014;15(6):739–45.
29. Kaza RK, Platt JF, Goodsitt MM, Al-Hawary MM, Maturen KE, Wasnik AP, et al. Emerging techniques for dose optimization in abdominal CT. Radiographics. 2014;34(1):4–17.
30. Von Falck C, Galanski M, Shin H. Informatics in radiology: sliding-thin-slab averaging for improved depiction of low-contrast lesions with radiation dose savings at thin-section CT. Radiographics. 2010;30:317–26. https://doi.org/10.1148/rg.302096007.
31. Becce F, Ben Salah Y, Verdun FR, Vande Berg BC, Lecouvet FE, Meuli R, et al. Computed tomography of the cervical spine: comparison of image quality between a standard-dose and a low-dose protocol using filtered back-projection and iterative reconstruction. Skeletal Radiol. 2013;42(7):937–45.
32. Omoumi P, Verdun FR, Ben Salah Y, Vande Berg BC, Lecouvet FE, Malghem J, et al. Low-dose multidetector computed tomography of the cervical spine: optimization of iterative reconstruction strength levels. Acta Radiol. 2014;55(3):335–44.
33. Geyer LL, Körner M, Hempel R, Deak Z, Mueck FG, Linsenmaier U, et al. Evaluation of a dedicated MDCT protocol using iterative image reconstruction after cervical spine trauma. Clin Radiol. 2013;68(7):391–6.
34. Tobalem F, Dugert E, Verdun FR, Dunet V, Ott JG, Rudiger HA, et al. MDCT arthrography of the hip: value of the adaptive statistical iterative reconstruction technique and potential for radiation dose reduction. AJR Am J Roentgenol. 2014;203(6):W665–73.